FLOW DISTRIBUTION IN A HERRINGBONE MICROFIN EVAPORATION TUBE

S. Wellsandt, Ph.D., Heat and Power Technology, Department of Chemical Engineering and Environmental Science, Chalmers University of Technology, Gothenburg, Sweden, Alpha Solutions AB, Gothenburg, Sweden, Sven.Wellsandt@alphasolutions.se

ABSTRACT

An experimental investigation of in-tube evaporation of R134a, R410A and R407C has been carried out for a 4 m long herringbone microfin tube with an outer diameter of 9.53 mm. Local circumferential wall temperatures are measured in ten sub-sections. The objective of the work was to determine the specific flow distribution caused by the herringbone structure and to compare measured results to reported results for helical microfin tubes. Also distribution differences between the pure fluid R134a and mixtures R407C and R410A at similar evaporation temperatures should be studied. Generally the herringbone tube shows wall dry-out at vapour qualities between 50-60%, which is lower than reported for helical microfin tubes, where local dry-out usually occurs at vapour qualities around 80%. The effect of swirl flow, characteristic for helical microfins, is non-existent in herringbone tubes. The V-shaped grooves in herringbone tubes combined with vapour density effects result in a rather complex flow pattern situation, which is discussed. It is also shown that the herringbone structure orientation plays an important role for the liquid film distribution and heat transfer in the investigated herringbone tube.

Key Words: ***herringbone microfins, wall temperature, R134a, R410A, R407C, flow pattern.***

1 INTRODUCTION

1.1 General

Measures for the protection of the stratospheric ozone layer as well as the global warming issue have led to the phase out of all chlorinated compounds including hydrochlorofluorocarbons (HCFCs). Chlorine-free compounds, such as hydrofluorocarbons (HFCs) and their mixtures have been proposed as substitutes for HCFCs. R-22, which plays an important role in residential, unitary and commercial air-conditioning applications has widely been replaced by refrigerant mixtures like R-407C, which has a theoretical COP close to that of R-22 and a very low global warming potential. However, the zeotropic characteristic of mixtures like R-407C has some implications for practical use, and one of the most severe problems is the heat transfer degradation during evaporation and condensation due to mass transfer resistance. Earlier investigations, like the one by Ebisu and Torikoshi (1995), show that the cross-counter air flow heat exchanger performance for R-407C is approximately consistent with that for R-22, when the advantage of temperature glide is well-matched with the disadvantage of heat transfer degradation. When a cross-parallel airflow configuration is applied, R-407C is significantly inferior to R-22. Thus they conclude in their paper that the successful application of R-407C in practical air conditioner requires heat transfer enhancement inside the heat transfer tube. For the purpose of heat transfer enhancement, new types of heat transfer tubes such as the helix, cross-grooved and herringbone microfin tube have been developed. Experimental data on the latter tube have been reported since 1996 and it was found to behave superior to the conventional helical micro fin tube depending on the refrigerant mass velocity. Yet the heat transfer enhancement mechanism has not been clearly explained and more experimental investigations are needed. Very little work has been published on the subject of flow distribution in a herringbone microfin tube. Wellsandt and Vamling (2003) presented a work on wall temperature measurements in a herringbone microfin tube, where they demonstrated a measurement technique with a high accuracy and a high degree of repeatability (precision), which promised reliable measurements and possible conclusions upon the specific flow distribution in a herringbone tube. The present work is a follow-up to the latter paper and shows results for R134a, R407C and R410A. Since herringbone microfin tubes and helical microfin tubes are often used for the same applications, differences in flow distributions using the respective structures are discussed.

1.2 Microfin Structures

Figure 1 depicts a schematic of geometric parameters used to characterise microfin tube features. Fins may be rectangular, trapezoidal or triangular. Major fin geometrical parameters of microfin tubes are the outer diameter d_o, the root diameter d_r, the fin height l, and the apex angle α. Other characteristic dimensions of microfin tubes are the helix angle β of individual fins with respect to the tube axis, the number of fins (or grooves) N_{gr} around the circumference in a tube, and the ratio of surface area of the microfin tube to that of a smooth tube if the microfins were removed (generally from 1.5 to 1.7). The fin pitch $p = (\pi\, d_{min}/N_{gr})$ is sometimes reported instead of the number of fins N_{gr}. Tubes with N_{gr} = 50-70, having fins with l = 0.075-0.4 mm and β = 10-30°, are commonly referred to as microfin tubes, while tubes with fewer (N_{gr} < 30) and taller fins (l > 0.4 mm) are referred to as internally finned tubes.

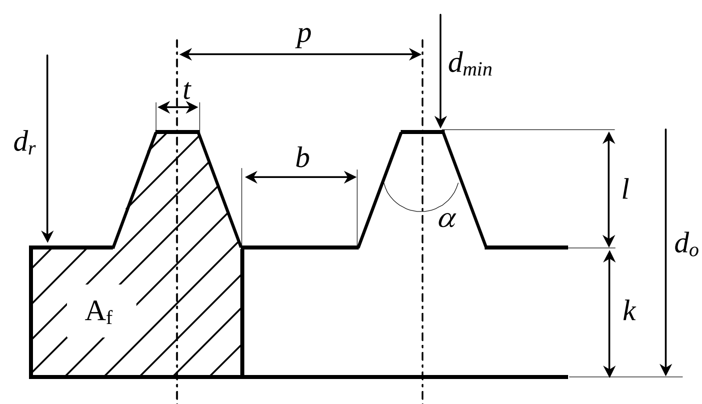

Fig. 1. Schematic of the microfin geometry

Note that parameters given above are applied in the same way for different microfin patterns, such as the helical microfin or herringbone microfin geometries shown in Fig. 2. To avoid any confusion, in this work they are always referred to as **helical microfin tube** and **herringbone microfin tube**. Below the herringbone microfin tube investigated in this study will be described in detail.

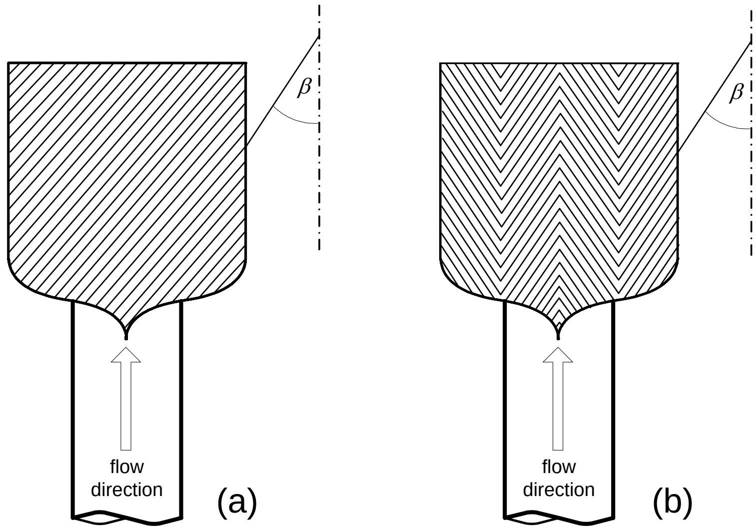

Fig. 2. Helical (a) and herringbone (b) microfin structures

Tatsumei and Ooizumi (1985) describe a number of early microfin tube manufacturing techniques, and Chiang (1993) relates that the microfin popularity has grown because of the significant enhancement of heat transfer, typically equal to or greater than the enhanced smooth tube surface area ratio. An additional benefit of the microfin tube is that pressure drops are generally higher by just 20% or less compared to smooth tube pressure drops.

Much effort has been put into the development of new fin shapes, and up to the 1990s helical microfin tubes have been improved by changing the fin and groove geometry from triangular to trapezoidal and by enlarging the fin height. The capacity of industry to develop new microfin structures seems to outpace the development of phenomenological models, which benefit the understanding of enhancement effects. While much work is required in order to improve our understanding of microfin tube effects in phase-change applications, continued development of new geometrical configurations will further enhance performance, Newell and Shaw (2001).

2 EXPERIMENTAL WORK

2.1 The Herringbone Microfin Tube Studied

The herringbone tube investigated has a pair of groove patterns on the inside. During the fabrication process the herringbone structure is rolled onto copper strip; then the strip is formed into a tubular shape, and finally the tube is welded longitudinally along its seam.

The tube configuration and tube specifications are given in Fig. 2 and Table 1 respectively.

Table 1. Tube specifications (perpendicular to fin)

d_o	9.53	mm
k	0.29	mm
l	0.212	mm
p	0.386	mm
t	0.096	mm
b	0.196	mm
α	25	°
β	16	°
N_{gr}	70	
area ratio	1.84	
weld orientation	bottom	

2.2 Experimental Apparatus

An overall schematic of the experimental apparatus is shown in Fig. 3.

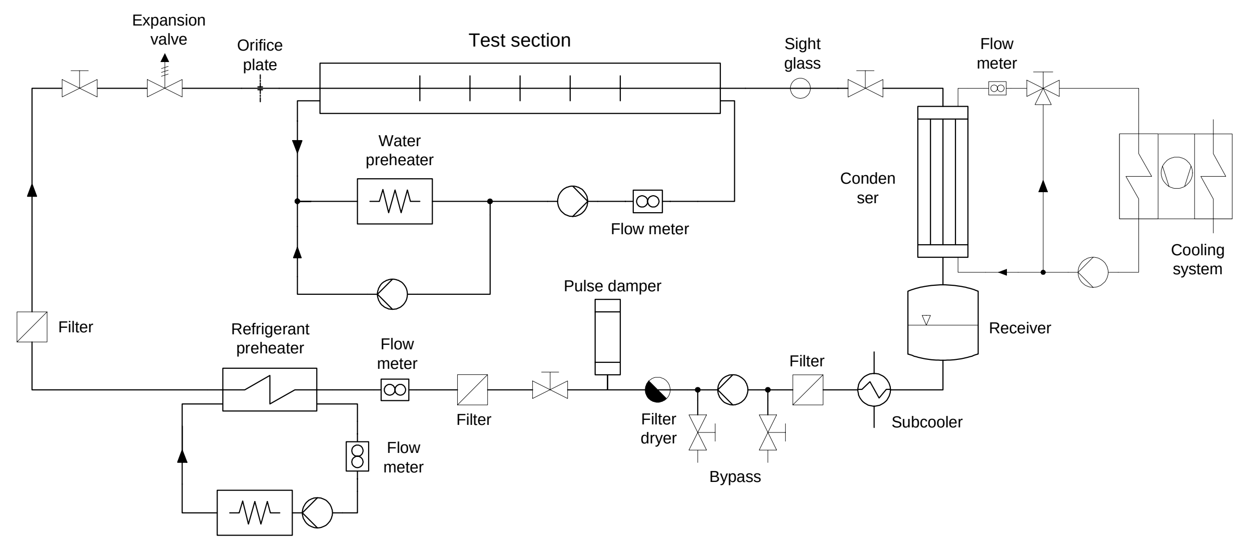

Fig. 3. Experimental apparatus

The set-up consists of four main flow loops: the refrigerant loop, the water loop, the preheater loop and the condenser loop. Main parts of the refrigerant loop are a preheater, an expansion valve, the test evaporator, a condenser, a coriolis-type mass-flow meter and a high-pressure pump. The latter enables measurements without presence of compressor oil.

The test section consists of a horizontally installed evaporator with a length of about four metres. The working fluid is introduced into the evaporator through an expansion valve, where the fluid is instantaneously evaporated to a vapour quality between 8% and 20%. In order to measure quasi-local heat transfer coefficients and wall temperatures, the evaporator is divided into ten subsections with an effective heat transfer length of 0.38 m each.

2.3 Wall Surface Temperature Measurements

The measurement method together with an error analysis and a discussion of resulting accuracies is given in Wellsandt and Vamling (2003), and only a short description of the method is included here.

There is no easy method of attaching a thermocouple to a surface so that it can be guaranteed to indicate the true surface temperature. To do this, it would be necessary to mount the measuring junction so that it could attain but not affect the surface temperature. In most cases, the presence of the thermocouple will cause a perturbation of the temperature distribution at the point of attachment, and thus it will only indicate the perturbed temperature.

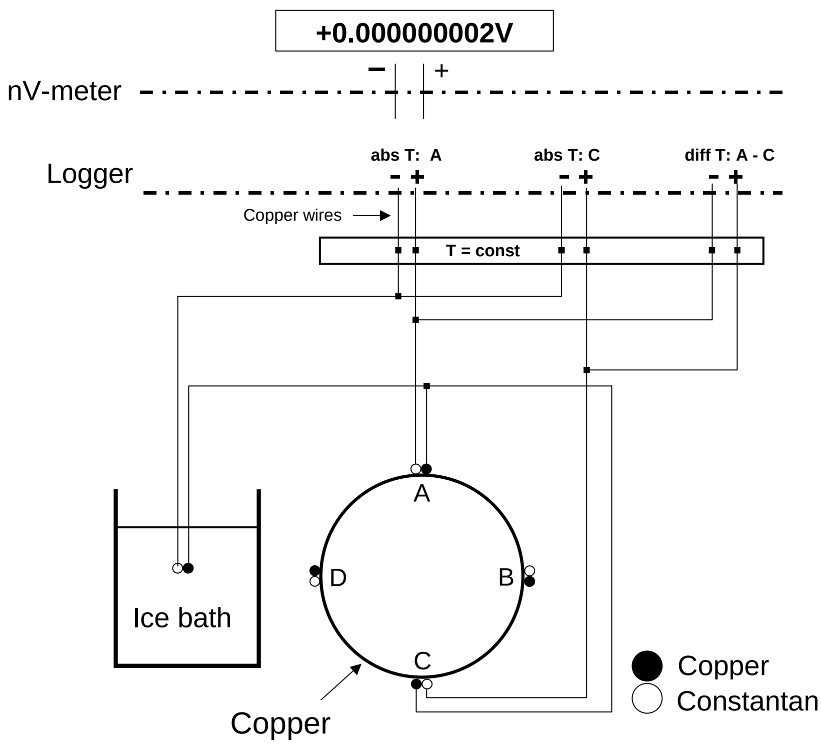

Fig. 4. Wall temperature measurement

Figure 4 shows the arrangement applied for wall temperature measurements. The extremely thin wall of the investigated tube does not allow installation methods such as fitting the thermocouple in a groove. Instead, very thin (∅ 0.2 mm) single copper and constantan wires were laser-welded onto the surface at the top, bottom and both sides. This allows exact placement of the wires, avoids the use of additional material, and guarantees a good thermal contact between the wire and the surface.

The absolute wall temperature can be determined at respective positions by connecting a constantan-copper pair (forming a thermocouple) to an ice bath and a voltmeter. Then the absolute wall temperatures at a second position can be determined by direct difference measurement. When measuring for example the temperature difference between top and bottom (A-C), the constantan wire and the copper surface at respective points are utilized as thermocouples. For this purpose the constantan wires at point A and point D are connected to the voltmeter. This way of measurement gives the advantage that even if slightly shifting evaporation conditions occur, i.e. a point with constant vapour fraction to some extent oscillates along the tube, these changes can be quantified. Absolute temperature measurements, which are read in a logging sequence, will in contrast be subject to a time delay.

For the absolute temperature measurement the bottom location was chosen, since this is presumably the most stable point considering liquid film thickness and local dry-out phenomena. However, the reference point can be moved at any time when needed, for example when the tube is rotated in order to investigate different structure orientations.

3 RESULTS

In contrast to the helical microfin structure, the nature of the herringbone pattern makes different orientations of the structure possible. Installed horizontally, the herringbone tube can be rotated such that diverging fins are placed at both sides, Fig. 5 (I), or at the top and the bottom of the tube, Fig. 5 (II), with positions between these two extremes being possible as well. The structure orientation (I) seems to be the "standard" installation for herringbone tubes at the present time, and hence most experiments were performed with the "standard" orientation in this work. However, the test section was constructed in such a way that a 90° rotation of the tube is possible, and some experiments with the "odd" orientation (II) have been carried out (see further below).

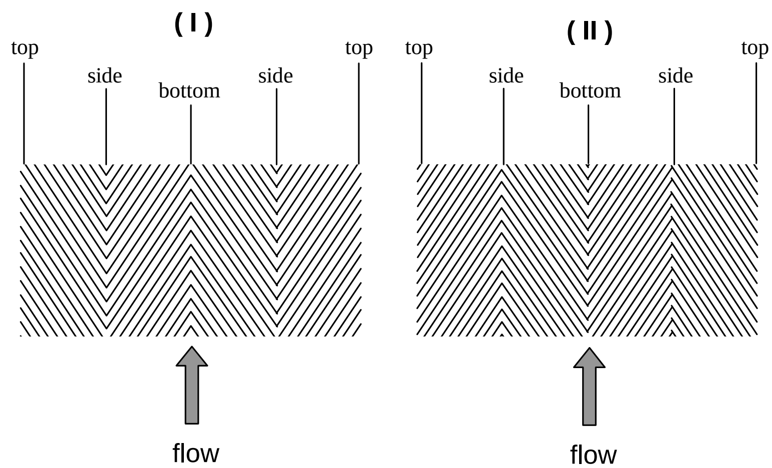

Fig. 5. Structure orientations investigated

3.1 Results Orientation (I)

Figure 6 depicts measured wall temperatures for two mass flow rates, G = 230 kg m^{-2}s^{-1} and G = 365 kg m^{-2}s^{-1}. Considering the lower mass flow rate case, it is noticeable that local circumferential wall temperatures for R410A show larger variations than for the other two fluids. This indicates differences in circumferential heat transfer caused by specific liquid film distribution as well as turbulence induced by vapour velocity and/or local herringbone structure. Generally, vapour velocities are between 50% and 90% higher for R134a than for R410A, and 10% to 20% higher for R407C compared to R410A. This might result in considerable differences in circumferential film thickness distribution, interfacial turbulence and even flow regimes. Where wall temperatures are higher at the top or at the sides of the tube than at the bottom, it is likely to be a sign of dry fin tips or parts of the tube perimeter. This results in poorer heat transfer compared to the bottom, where the entire surface is likely to be covered by liquid. Both R410A and R407C show this even for low vapour qualities, whereas R134a produces higher wall temperatures at the bottom than at the top. The latter suggests that for R134a the whole perimeter is covered by liquid with the thickest film at the bottom and thinnest film at the top. For higher vapour qualities, starting at x = 0.6, R134a shows an increasing wall temperatures indicating dry parts. Here the high vapour velocity probably causes a certain amount of liquid to be sheared off the wall.

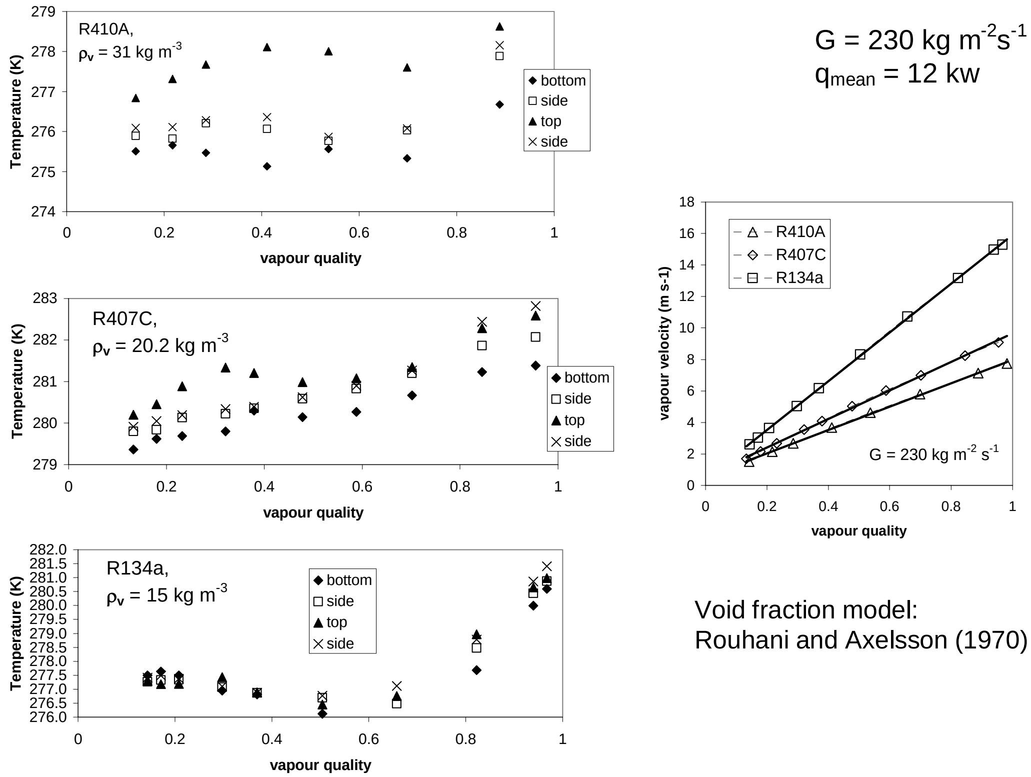

Fig. 6. Measured wall temperatures for G = 230 kg $m^{-2}s^{-1}$

The high mass flow rate case, depicted in Fig. 7, shows a different picture. Local wall temperatures do not show the same large variation, and top-wall temperatures move more towards side-wall temperatures. One possible interpretation is that higher velocities result in a more even circumferential film thickness.

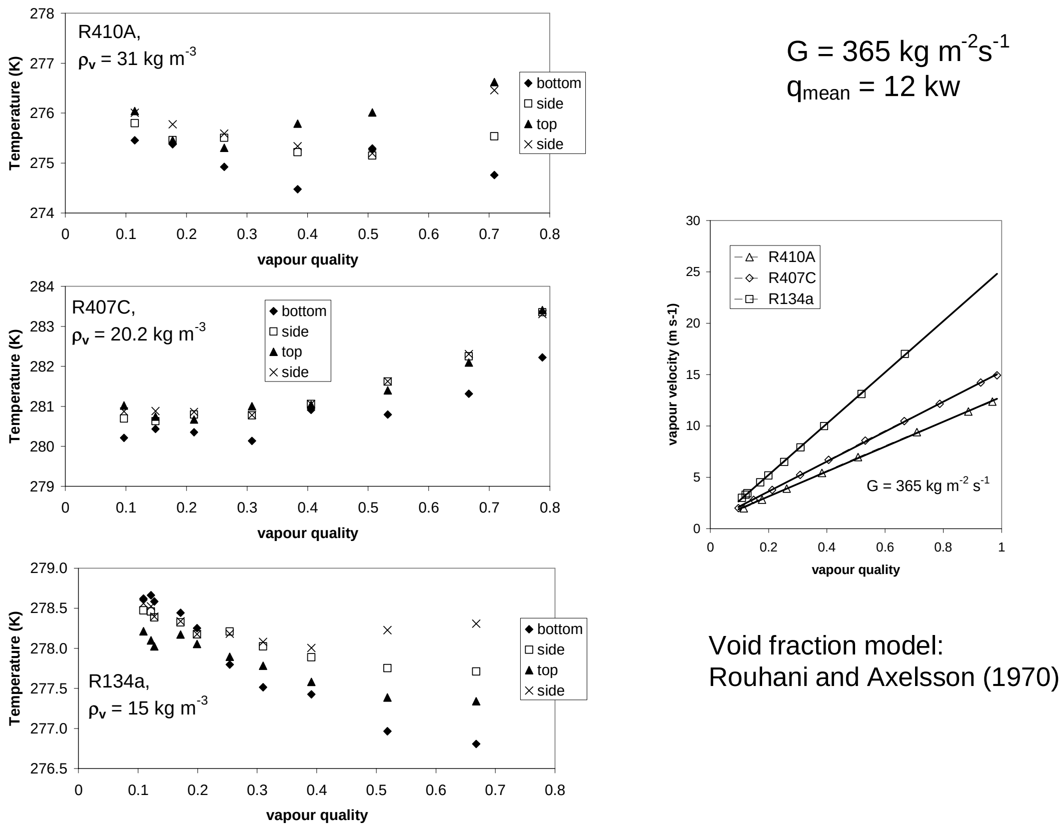

Fig. 7. Measured wall temperatures for G = 365 kg m^{-2}s^{-1}

3.2 Results Orientation (II)

At the present time no experimental work on the effect of different structure orientation during evaporation is reported. Thus a test series with R407C has been carried out in order to investigate whether or not heat transfer in the present herringbone microfin tube depends on structure orientation.

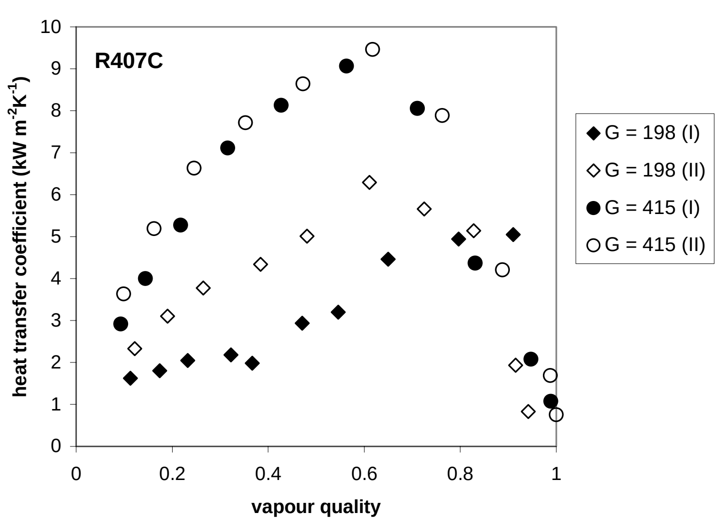

Fig. 8. Effect of structure orientation

Figure 8 shows clearly that structure orientation (II) yields higher heat transfer coefficients at lower flows (G = 198 Kg m^{-2}s^{-1}), whereas there is no difference between the two structure orientations at high flow (G = 415 Kg m^{-2}s^{-1}). This result is rather surprising, since orientation (I) seems to be the "standard" installation for herringbone tubes at the present time.

For the two mass flow cases in Fig. 8, measured wall temperatures are depicted in Fig. 9 and Fig. 10 respectively. For additional information, also refrigerant temperatures and heat fluxes are included in the figures. In Fig. 9 it is seen that wall temperatures for structure orientation (I) show a larger circumferential variation than for orientation (II). This indicates that, at lower mass flow rates, orientation (II) produces a more even film, with the whole perimeter covered by liquid, whereas orientation (I) does not. Below 60% vapour quality, better heat transfer for orientation (II) leads both to a lower mean wall temperature (i.e. smaller temperature driving force) and higher heat flux.

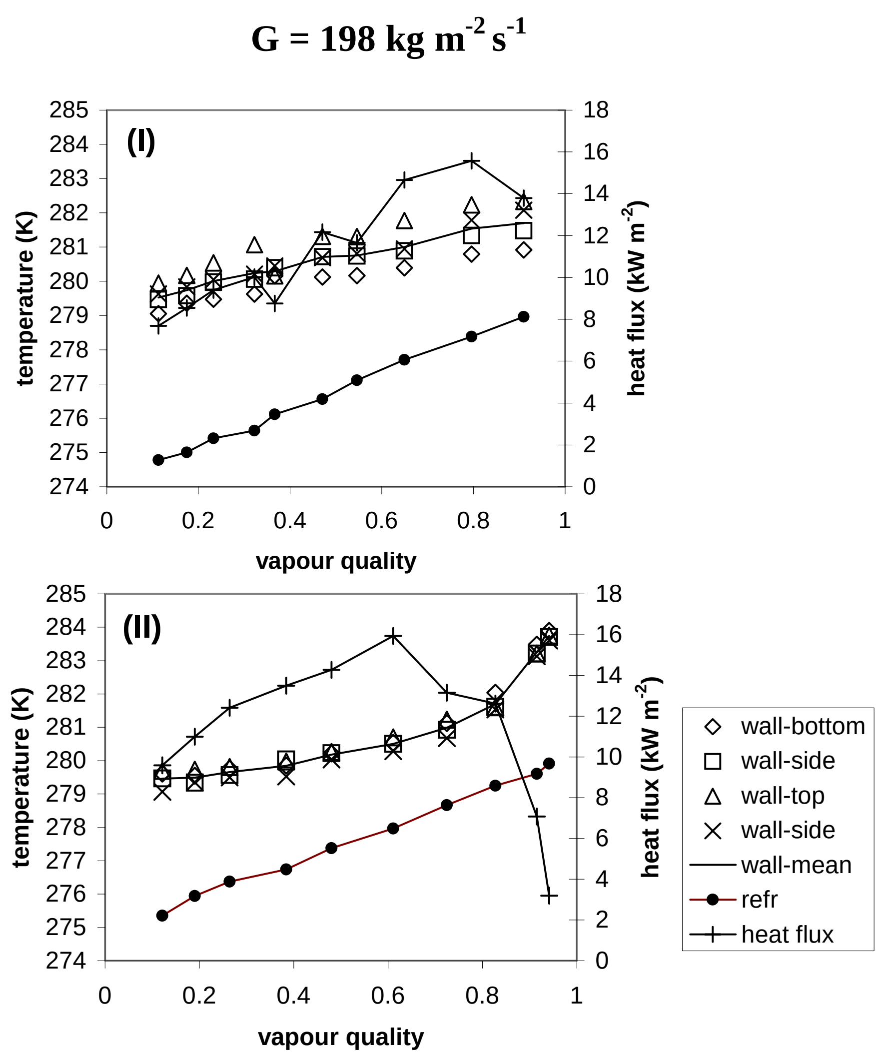

Fig. 9. Wall temperatures for structure orientations (I) and (II) at G = 198 kg m^{-2}s^{-1}

For the high mass flow rate case, Fig. 10, the mass flow rate effect seems to overwhelm the structure orientation effect. Both orientations seem to produce comparatively even film distributions, leading to equally effective heat transfer. Mean wall temperatures, resulting temperature-driving forces and also heat fluxes are about the same.

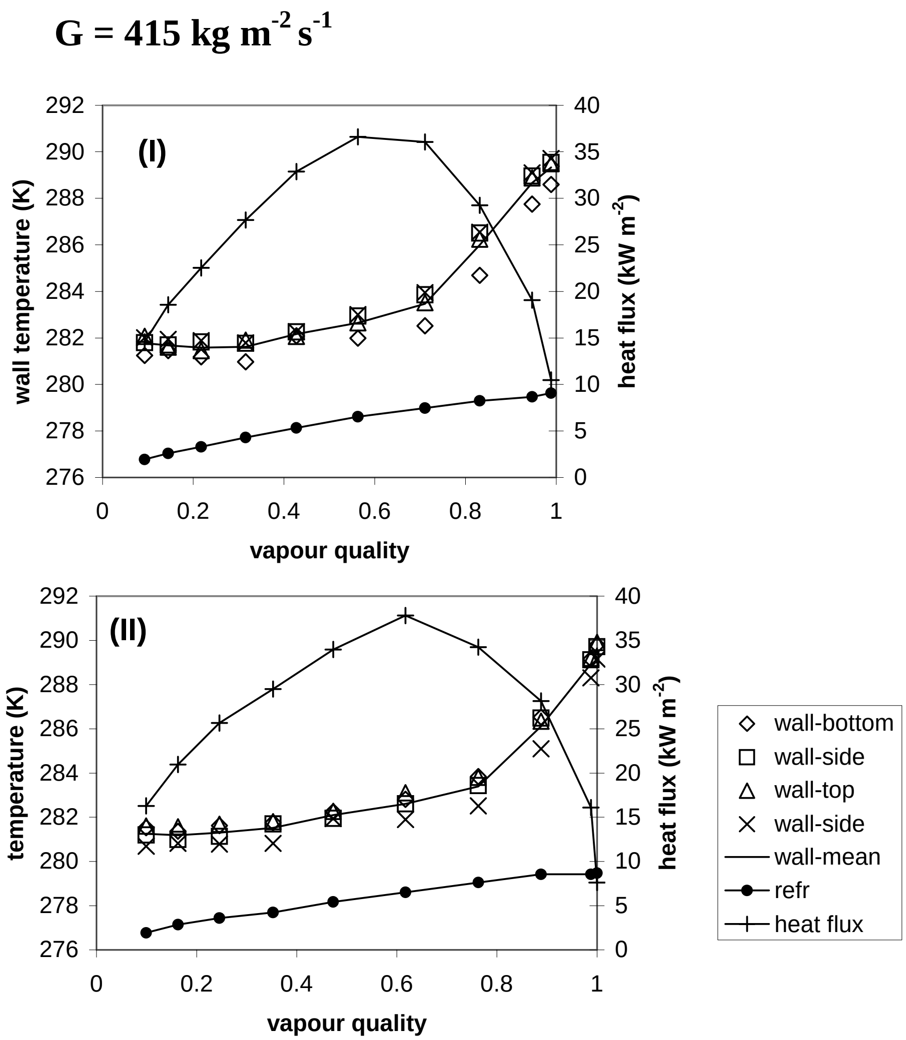

Fig. 10. Wall temperatures for structure orientations (I) and (II) at G = 415 kg m^{-2}s^{-1}

4 DISCUSSION

4.1 General

When comparing results from the present work to results from other works on microfin tubes one should keep in mind the differences between short and long test-sections. The long test section in this work is very beneficial because one is able to obtain local heat transfer measurements while at the same time incorporating the possible complex effects that occur due to multiple flow regimes occurring simultaneously in the test section; the latter is a more realistic case than the shorter test sections usually studied. However, it should be pointed out that the temperature profile on the water side not exactly reproduces the boundary conditions found in fin and tube heat exchangers. Fairly constant air temperatures at each column of tubes are found there.

4.2 Wall Temperatures

The heat transfer peak at lower vapour qualities is usually not observed in helical microfin tubes. Koyama *et al.* (1995) and Thome *et al.* (1997) show flow boiling results for R134a produced with a helical microfin tube in a six- and a three-metre long test tube respectively. Both report an increase of heat transfer coefficients up to 80% vapour quality. This indicates that wall dry out does not occur below this vapour quality. Test with clear PVC tubing with a helical microfin pattern, performed by Shedd and Newell. (2003), show annular flow up to a vapour quality of 76 %. This raises the question of main differences between herringbone and helical microfins and how they influence two-phase flow boiling. Based on the analysis of independent studies on helical microfin tubes, Thome (1996) states a number of heat transfer augmentation mechanisms. Effects like an increase of the liquid-only heat transfer coefficient, or the creation of additional nucleation sites by partially shielding them should occur both in helical and in herringbone microfin tubes. However, the effect of swirl flow occurring in helical microfin tubes, which shifts the onset of partial dryout at the top of the evaporation tube to higher vapour qualities, is non-existent in herringbone tubes. Instead, as a consequence of the V-shaped grooves, there is a particular wetting in two directions. Converging fins at the top and bottom of the tube might cause a higher degree of turbulence, since liquid is forced over subsequent fins like over a corrugated plate. This may increase the liquid-only heat transfer, but could also cause a certain amount of liquid to be sheared off the wall, especially when vapour velocities increase. At the sides of the tube, where fins diverge, a substantially thinner liquid film should increase heat transfer. However, Rudy and Webb (1985) show in their work on condensate retention on horizontal integral-fin tubes that surface tension drains the fins. Gregorig (1954) first described the effect that the interaction of convex and concave surfaces creates a surface tension force that draws liquid from the convex surface to the concave region. Rudy and Webb state that the fin profile does not need to have a special shape for surface tension drainage to occur. Expanding this theory to evaporation, and taking into account that there is no continuous condensation rate to the fin top in order to maintain a liquid film, it is very likely that the described effect causes the upper part of the fin to dry out.

In earlier investigations of microfin herringbone tubes, such as the one performed by Ebisu and Torikoshi (1998), a herringbone specific flow distribution with thinner liquid films at both sides than at the top and bottom of the tube is suggested for a vapour quality range between 20% and 80%. This cannot be confirmed with the present work. In order to draw more confident conclusions about local flow distribution, techniques more sophisticated than wall measurements are needed. Indirect flow pattern observations like the present one always include the risk of miss-interpretation. For example could high wall temperatures be a sign of a thick liquid film but also an indication of dry fin tips.

Finally it should be mentioned that the geometry and location of the weld is not investigated here. Thus the effect of weld geometry and location should be part of future investigations.

5 CONCLUSIONS

The present work is to be placed at the beginning of the long path to understanding the flow distribution in herringbone microfin tubes. It gives indications for the complexity of flow patterns in herringbones tubes compared to helical microfin tubes. In the absence of swirl flow in a herringbone tube a continuous wetting of the tube's perimeter seems less likely to be established. A consequence of lower vapour velocities at low vapour qualities is that a liquid film at the top of the tube cannot be maintained. On the other hand may higher vapour velocities at high qualities increase the risk for the liquid to be sheared off. Thus the refrigerant vapour density is an important factor to consider.

A specific flow distribution with thinner liquid films at both sides than at the top and bottom of the herringbone tube suggested in earlier investigations cannot be confirmed in the present work.

Different structure orientations were tested and it was found out that the less common orientation, i.e. diverging fins are placed at the top and the bottom of the tube, produces a more uniform liquid film at a lower mass flow rate. At a high mass flow rate no difference was found for the investigated orientations.

REFERENCES

Chiang R. 1993. “Heat transfer and pressure drop during evaporation and condensation of Refrigerant-22 in 7.5 mm and 10 mm diameter axial and helical grooved tubes”, *Proc. AIChE Heat Transfer Symposium*, (89)29: pp. 5205-10.

Ebisu T., K. Torikoshi 1998. “Experimental study on evaporation and condensation heat transfer enhancement for R-407C using herringbone heat transfer tube”, *ASHRAE Transactions*,104, Pt.2.

Gregorig R. 1954. “Film condensation on finely rippled surfaces with consideration of surface tension”, *Z. Angew. Math. Phys*, 5: pp. 36-49.

Koyama S., J. Yu, S. Momoki, T. Fujii, H. Honda 1995. “Forced convective flow boiling heat transfer of pure refrigerants inside a horizontal microfin tube”, *Proc. Convective Flow Boiling*, Alberta, Taylor & Francis; pp. 137-142.

Newell T.A., R.K. Shah 2001. “An assessment of refrigerant heat transfer, pressure drop and void fraction effects in microfin tubes”, *Int J of Heating, Ventilation, Air-Conditioning and Refrigerant Research*, Vol 9(2), pp. 125-153.

Rudy T.M., R.L. Webb 1985. “An analytical model to predict condensate retention on horizontal integral-fin tubes”, *J Heat Transfer*, 107: pp. 361-368.

Shedd TA, Ty. A. Newell 2003. “Visualization of two-phase flow through microgrooved tubes for understanding enhanced heat transfer”, *Int J Heat and Mass Transfer*,46: pp. 4164-4177.

Tatsumei A., K. Ooizumi 1985. “Grooved tubes for air conditioners”, *Tube International*, pp. 162-166.

Thome J.R. 1996. “Boiling of new refrigerants: a state-of-the-art review”, *Int J Refrigeration*, 19(7), pp. 435-457.

Thome J.R., N. Kattan, D. Favrat 1997. “Evaporation in microfin tubes: a generalized prediction model”, *Proc. Convective Flow and Pool Boiling Conf., May 18-23*, Kloster Irsee, Paper VII-4.

Wellsandt S., L. Vamling 2003. “Wall temperature measurement in a herringbone microfin evaporation tube.” *Proc. International Congress of Refrigeration*, Washington D.C., USA.